




EVALUATION OF THE EFFECT OF LUMINOSITY ON CERAMIC MICROBIAL FUEL BIOCELLS WITH SPHAGNUM MOSSES USING A LOW-COST HYDROGEL-BASED CATHODE FROM FE-N-C

 <https://doi.org/10.56238/levv16n46-045>

Submitted on: 12/02/2025

Publication date: 12/03/2025

Maria Isabela Alves Antunes¹, Gustavo Pio Marchesi Krall Ciniciato²

ABSTRACT

The text discusses the growing demand for electricity and the need for sustainable sources. The use of fossil fuels has generated significant environmental impacts, such as the emission of greenhouse gases. Fuel cells emerge as an efficient and clean solution, but they face challenges such as high costs and sensitivity to contaminants. Fuel biocells, using biological catalysts, present a more sustainable and cost-effective alternative. Despite their benefits, biocells still face limitations in terms of efficiency and durability.

Keywords: Fuel cells. Fuel cell biocells.

¹ Federal Institute of Education, Science and Technology of São Paulo, Avaré Campus – São Paulo
Isabela.maria@aluno.ifsp.edu.br

² Prof. Dr.

Federal Institute of Education, Science and Technology of São Paulo, Avaré Campus – São Paulo
gustavo.ciniciato@ifsp.edu.br

INTRODUCTION

Energy is one of the fundamental pillars of social development. The growing global interconnection and diversity of electronic devices have driven an ever-increasing demand for electrical energy. In Brazil, the national consumption of electricity reached 46,314 GWh in February 2024, registering an increase of 8.0% compared to the same month in 2023. This value represents the fourth highest monthly consumption in the entire time series, which began in 2004. In this context, emerging technologies aimed at the production of renewable and clean energy become increasingly relevant.

Traditional power plants have predominantly used fossil fuels for electricity generation for decades. The large-scale burning of these fuels results in significant environmental impacts, such as the emission of large amounts of greenhouse gases (GHG), the degradation of the ozone layer, the worsening of global warming, the accelerated melting of polar ice caps, and the rise in sea levels (SANTOS et al., 2023). These effects highlight the urgency of transitioning to more sustainable energy sources.

In the face of these challenges, the search for alternative energy sources has intensified to diversify the global energy matrix and, above all, minimize the environmental impacts associated with energy production. The UN 2030 agenda, through Sustainable Social Development Goals (SDG) 7, highlights an action plan to ensure reliable, sustainable, modern, and affordable access to energy for all (UN, 2015).

While renewable energy sources such as wind, solar, geothermal, and tidal energy play an increasingly important role in providing sustainable energy to homes, they face limitations in applications that require mobility or operation in off-grid locations. These technologies, while effective for large installations, are not always feasible for handheld devices or stand-alone systems. In this scenario, fuel cells emerge as an innovative and practical solution, capable of converting chemical reactions into electricity efficiently and sustainably, overcoming some of the barriers of traditional renewable sources.

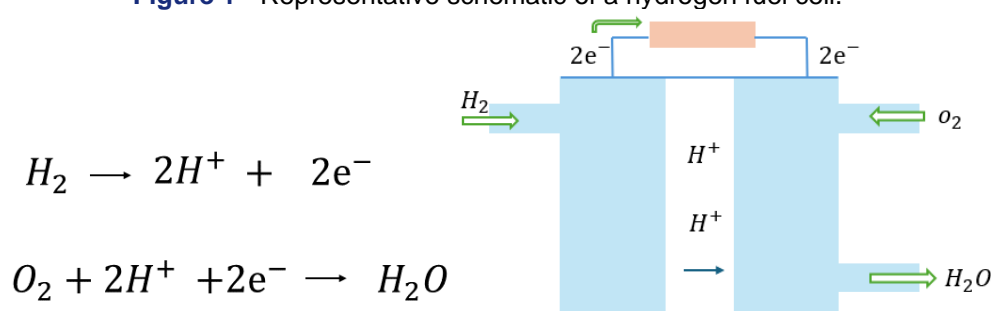
FUEL CELLS

Fuel cells can help reduce our reliance on fossil fuels and decrease harmful emissions to the atmosphere since fuel cells theoretically have higher electrical efficiencies compared to heat engines. This technology consists of the conversion of chemical energy into electrical energy, operating in a similar way to the batteries present in society's daily life, that is, a pair of oxidation-reduction reactions producing electric current with enough electrical energy to supply portable electronic equipment. However, there is a difference,

since, while in the cell or battery, the fuel and oxidizer are stored within the system, in fuel cells (CaC), the reactants can be added externally (Carrette et al., 2001).

Fuel cells are an energy conversion system that has as its operating principle the electrochemical combustion of a fuel and the electrochemical reduction of an oxidizer. In its basic configuration, a fuel cell consists of two electrodes, whose composition depends on the type of cell, separated by an electrolyte that enables ion conduction and connected using an external circuit, which enables electrical condition. The electrodes are exposed to a flow of gas or liquid to supply the reactants, being the fuel and the oxidizer (Wendt et al., 2000). A schematic of a hydrogen fuel cell is depicted in Figure 1.

Figure 1 - Representative schematic of a hydrogen fuel cell.



Source: Authorship, 2025.

Fuel cells are classified using the electrolyte as a reference criterion. Thus, phosphoric acid, alkaline solid polymeric electrolyte cells, molten carbon, and solid oxides cells stand out (Ticianelli and Gonzalez, 1988).

The first applications of CaCs consisted of the North American space program in which space vehicles used pure hydrogen as fuel. The terrestrial applications of this system began to happen with the advent of the oil crisis in 1973 (Gonzalez, 2000).

When hydrogen is used as a fuel, the byproducts of the reaction are heat and pure water, which means that the fuel cell can be seen as having a zero-emissions technology. Direct energy conversion and lack of mechanical movement inside the stack can lead to highly safe and long-lasting systems. However, what makes the use of fuel cells difficult today is the high cost of the noble materials that make up the catalyst. In addition, the production of hydrogen resorts to intensive use of energy and often derives from fossil fuels (Santos, 2004). In addition, it needs to be free of certain nitrogen and sulfur contaminants, which are usually present when hydrogen is produced by biogas reforming. These contaminants, when they come into contact with the catalyst of a cell that contains platinum in its composition, end up poisoning the surface of this noble metal, causing it to stop working.

In this context, fuel cells offer several advantages, such as clean energy generation and efficiency in specific applications. However, its implementation is still unfeasible due to high costs and sensitivity to contaminants, which can compromise the performance of catalysts. Given these limitations, fuel biocells emerge as a promising alternative, taking advantage of biological processes that already occur naturally to produce energy more sustainably and economically.

SOIL BIOFUEL CELLS

Due to the challenges faced by conventional fuel cells, biological fuel cells have attracted increasing interest and attention. Unlike fuel cells, fuel biocells are a device that can employ both mobilized enzymes, called an enzymatic biofuel cell (ECB), and microorganisms, known as a microbial biofuel cell (BCM), as a catalyst instead of the traditional noble metal catalysts (Neto and Andrade, 2013).

Biological catalysts for fuel biocells do not have the economic limitations and availability of noble materials such as platinum, once a microorganism or enzyme capable of oxidizing substrates and transferring electrons to electrodes with high efficiency is discovered, its demand is capable of meeting all the need and dependence on noble metals (Gomes, 2011). Another advantage to the use of these catalysts is the wide range of fuels that can be used and the low purification required (Shukla, 2004).

There are major differences in the use of enzymatic biofuel cells (BCE) and microbial biofuel cells (BCM), particularly in terms of application, efficiency, and durability. Enzymatic fuel biocells have been shown to have higher current and power densities, but are limited by incomplete oxidation of the fuel, in addition to the enzymes having a shorter activity period of 7-10 days, consequently having to be replaced (Cooney, 2008), enzymes are sensitive to changes in pH and temperature (Hanson, 2021). On the other hand, BCM offers greater stability and resistance to environmental changes, making it a more durable alternative (Cooney, 2008). Many microorganisms can completely oxidize their fuel (typically, lactate and glucose), but some microbial biofuel cells employ animal waste as fuel, while still others collect carbohydrates from sandy soils. However, BCMs are still limited by low current and power densities. In these cells, a microbial biofilm on the electrode can produce an electric current continuously, as long as minimum conditions are maintained for the survival of the microorganisms, allowing the natural regeneration of the system.

Highlighting BCM, the functioning of a bioelectrode in a BCM happens due to the transfer of electrons involved in the metabolism of the microorganism in contact with the

electrode. In evolution, living organisms have used the anaerobic process over millions of years, making use of various methods to reduce compounds for their cellular metabolism. Such bacteria were probably capable of using different types of electron acceptors (Mesquita, 2016). Among them, some were capable of transferring electrons out of the cell, directly to the external environment, called exoelectrogenic bacteria (Logan, 2008), which allows their use in microbiological fuel cells, as it is possible to establish electrochemical contact with the electrode (Logan and Regan, 2006). The exchange of electrons between the bacterium and the electrode occurs through three mechanisms: direct transfer, mediated transfer, and nanowires or pili (Schröder, 2007).

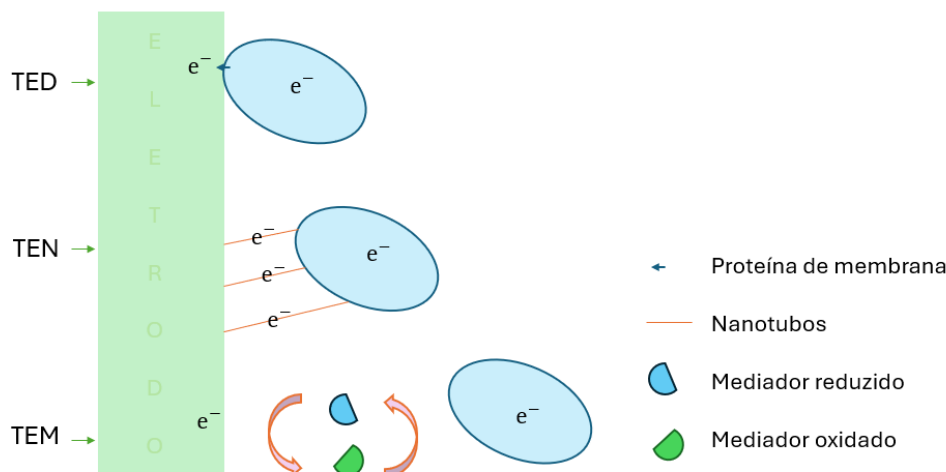
Direct electron transfer (TED) occurs through a physical contact of the bacterial cell membrane or a membrane organelle with the anode of the fuel cell, without involving the use of diffusional redox species in the transfer of electrons from the cell to the electrode (Schröder, 2007).

Some microorganisms can develop extensions of their cell wall (nanowires); this extension can communicate electrochemically with the external environment of the cell, consequently increasing the surface area of contact with the electrode and the transfer of electrons, in addition to having the function of adhesion to surfaces. Nanowires are structures that are part of the microorganism. They were identified in strains of *Geobacter sulfurreducens* and *Shewanella oneidensis*, which made a connection between the bacterium and the electrode (Gorby, 2006). This mechanism enables a transfer of electrons from a bacterium to the electrode without the need for mediators (Schröder, 2007).

For those microorganisms that do not have TED or TEN capability, there is the possibility of mediated electron transfer (TEM), which uses mediators to transport electrons. Mediators are chemical compounds that, when added to the system, promote reversible oxidation-reduction reactions, making it possible to exchange electrons between the bacterium and the electrode. The compound is absorbed by the bacterium in its oxidized form and passes inside it to the reduced form, capturing the electrons and transporting them to the outside of the cell until it meets the electrode, where it returns to its oxidized form, cyclically performing this procedure until the total consumption of the existing substrate by the microorganism (Teleken, 2013).

A schematic of the electronic transfer mechanisms in BCM can be seen in Figure 2.

Figure 2 - Electron transfer mechanisms in a microbial fuel cell biocell. From top to bottom: TED direct wire transfer, TEN nanowire wire transfer, and TEM mediated wire transfer.



Source: Authorship, 2025.

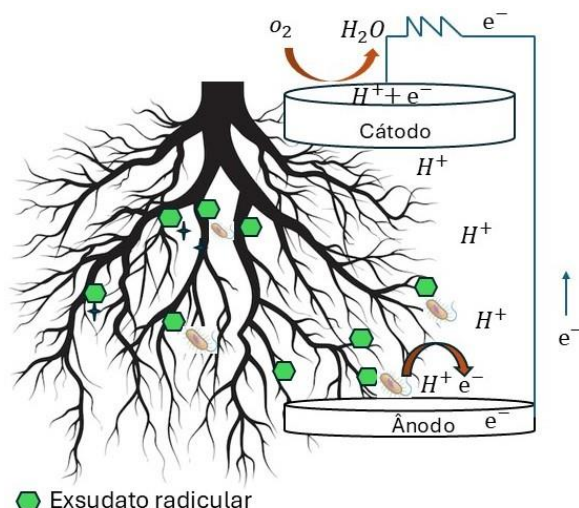
Understanding these mechanisms of electron transfer from bacterial cells to electrodes is of utmost relevance for the development of anodic materials that make the transfer as efficient as possible (Park and Zeikus, 2003).

There is a diversity of studies involving BCMs recorded in the literature. Highlighting the use of mixed cultures of exoelectrogenic microorganisms found in various anaerobic environments that allow the exchange of electrons with the external environment, this mixed culture popularly uses sludge from water treatment plants (Gul, 2021), seabed sediment (Moraes, 2016), and soil microorganisms (Oliveira, 2019).

The rhizosphere refers to the region of the soil influenced by the roots, with maximum microbial activity. Plant growth is controlled substantially by the soil in the root region, an environment that the plant itself helps to create and which is associated with microbial activity that exerts several beneficial activities. In terms of genetic diversity, the soil is the site of numerous and varied populations of all types of microorganisms (Zilli et al., 2003). All these characteristics mean that the root part of the plant must contain a considerable population of anaerobic and exoelectrogenic microorganisms, which makes it a promising environment for BCM construction.

Fuel biocells surrounding the rhizosphere have been studied for a short time. Its operation consists of an anode inserted inside a substrate near the rhizosphere and a cathode in contact with atmospheric oxygen, as shown in Figure 3.

Figure 3 - Representative scheme of rhizosphere-electrode interaction in a biofuel cell with soil microorganisms.



Source: Authorship, 2024.

Exoelectrogenic microorganisms present in the rhizosphere can convert the organic matter of root exudates, for example, into electrons and protons and CO₂. Studies involving BCM with the rhizosphere of bryophytes are known in the literature, also known as Photosynthetic Fuel Cell, since, in reality, the driving force of the entire process is sunlight (Shlosberg, 2023). The use of BCM involving soil microorganisms in contact with mosses is interesting, because, in addition to being pioneer plants, mosses can thrive in humid environments with high salt concentration, which is ideal for a microbial fuel biocell, despite not having a defined root, mosses have similar structures with the same functions, called rhizoid. A recent study proved that a BCM of *Physcomitrella moss* was able to generate 2.5 mW.m⁻², enough power to run small devices (Bombelli, 2016).

Recently, a study conducted by our group demonstrated that the rhizosphere of *Sphagnum* mosses produced electrochemically active compounds in a prototype ceramic fuel biocell using an optimal electrolyte of 100 mL KCl (Filho, 2023). Initially, the experiments investigated the influence of lighting time on BCMs, and the results proved that, yes, lighting time is the driving force of the system since photosynthesis needs to occur. Now, the focus is on the development of a catalyst based on Fe-N-C hydrogel incorporated into the cathode, aiming to improve the electrochemical performance of this technology. Thus, it is essential to carry out new experiments to evaluate the impact of this catalyst on the efficiency of the biocell.

CATHODES FORMED BY FE-N-C HYDROGEL

Biofuel cells represent a technological evolution based on the principles of conventional fuel cells. As a result, many of the techniques widely used in fuel cells end up

being adapted to biocells. However, the application of noble metals, such as platinum, faces critical challenges, including their high cost and vulnerability to inactivation by nitrogenous and sulfurous compounds often present in complex substrates used in microbial biocells.

A widely studied alternative to replace platinum in fuel biocells is the use of activated carbonaceous materials and graphite as the cathode. These materials, in addition to being low cost, have a high specific surface area, providing a greater number of active sites for the Oxygen Reduction Reaction (ROR). However, the oxygen reduction mechanism in these materials usually follows a 2-electron transfer pathway, which can result in a weak energetic interaction with the carbon surface (Deng et al., 2010). This characteristic leads to high polarization by activation, significantly reducing the performance of the microbial fuel biocell (BCM).

Currently, the most promising electrocatalysts for RRO are based on "co-doped" carbon catalysts of nitrogen and transition metal inserted into a carbon matrix that will be described as M-N-C (Oliveira, 2018). Given this, operations based on transition metal and nitrogen-doped carbon (M-N-C) emerge as a highly promising alternative. These materials combine the conductive properties of carbon with the catalytic activity of metals such as Mn, Co, Ni, Cu, and Fe, the latter being the most efficient metallic element in coordinating oxygen reduction reactions (ORR). This is due to its synergistic effect, which combines a high concentration of active sites with a porous structure, facilitating mass transport and improving catalytic performance (Mineva et al., 2019). In addition, recent studies corroborate that Fe presents a favorable electron configuration for the adsorption and activation of O₂ molecules, which is crucial for the efficiency of ORR (Lefèvre et al., 2020).

According to Genesan et al., iron atoms play an important role in the constitution of active sites, producing high activity for RRO when compared to electrocatalysts prepared without the addition of Fe as a transition metal.

Despite the variety of metals (M) that can be used as catalysts, Fe-N-C materials stand out for their combination of low cost and high functionality. Yang et al. (2019) demonstrated an affordable procedure for synthesizing these catalysts, utilizing chitosan gels as a nitrogen (N) source and ferric chloride (FeCl₃) as a Fe ion source. The results showed a 33% increase in electricity generation compared to systems that did not use the catalyst. Inspired by these advances, the present work aims to develop cathodes containing catalysts of Fe-N-C hydrogels, incorporate them into an electrochemical cell, and perform electrochemical experiments.

WORK OBJECTIVES

The objectives of this project stage are to perform electrochemical studies on microbial fuel biocells using *Sphagnum mosses* and to determine the effect of the insertion of the Fe-N-C hydrogel catalyst in the gas diffuser layer. For this, cathodes containing Fe-N-C hydrogels catalysts were developed and incorporated into the electrochemical cell.

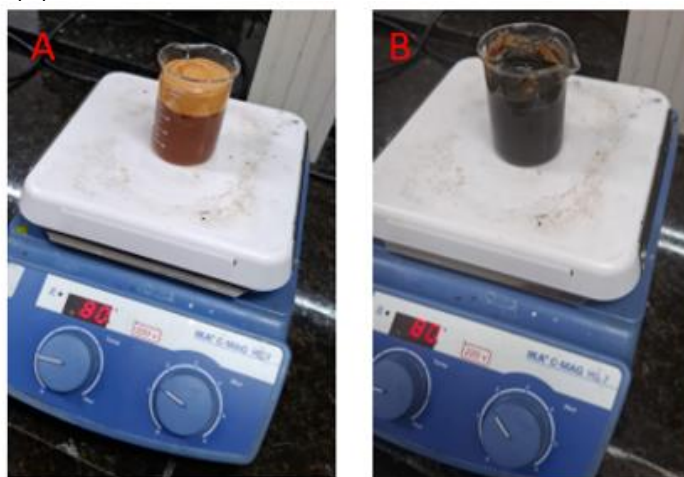
Cyclic voltammetry experiments were carried out in half a cell to obtain information about surface processes in the electrodes through analysis of the potential ranges in which the reduction and oxidation processes occur, both of the anode in contact with the ground and of the cathode containing the gas diffuser layer.

EXPERIMENTAL PROCEDURE

SYNTHESIS OF THE HYDROGEL CATALYST FE-N-C

For the synthesis of the Fe-N-C catalyst, the methodology of Yang et al. (2019) was followed by direct pyrolysis in an inert atmosphere. Initially, 1g of anhydrous FeCl_3 was dissolved and stirred for 10 minutes in 75 mL of deionized water. Then, 2 g of chitosan was gradually added to the FeCl_3 solution under constant stirring, maintaining the temperature at 80°C for 4 hours. After the mixture of chitosan with FeCl_3 was completed, 6 g of *black* carbon was added to it, which continued under agitation at 80°C for another 4 hours, as shown in Figure 4.

Figure 4 - Chitosan mixture in FeCl_3 solution at 80°C under stirring (A) and with black carbon added to chitosan-Fe(III) hydrogel (B).



Source: Authorship, 2025.

The mixture was then transferred to the vacuum drying oven, where it was maintained at 60°C and 300 torr pressure for a period of 12 hours (Figure 5).

Figure 5 - Chitosan-Fe(III) hydrogel and carbon in vacuum drying oven at 300



Source: Authorship, 2025.

After drying, the material was subjected to a heat treatment in an inert atmosphere furnace at 800°C for 15 minutes, under a nitrogen gas atmosphere, using a 10°C.s-1 heating ramp. The oven was purged with argon for 30 minutes before the beginning of the procedure and followed with argon being added throughout heating (Figure 6).

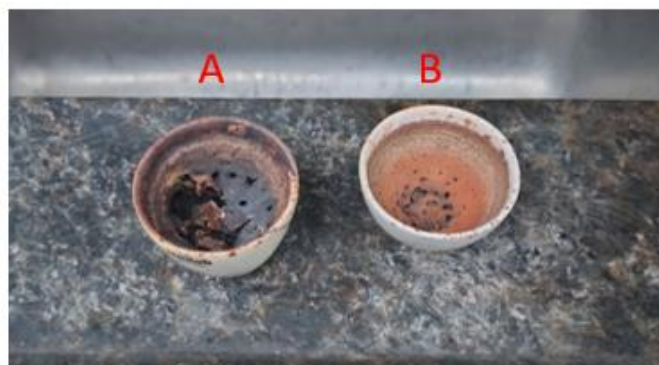
Figure 6 - Heating of the mixture in the inert atmosphere oven.



Source: Authorship, 2025.

The resulting powder was dissolved in a solution of 0.01 M HCl for a period of 1 hour to remove possible impurities. Then the material was washed 5 times with deionized water to completely remove waste. Finally, the material obtained was dried again in a vacuum drying oven at 60° C and 300 torr for a period of 6 hours. This product, called Fe-N-C hydrogel catalyst (figure 7), was used to treat the carbon tissue used as cathode.

Figure 7 - Fe-N-C hydrogel catalyst after heat treatment in an inert atmosphere (A) containing black carbon and (B) without black carbon.



Source: Authorship, 2025.

PREPARATION OF CATHODES CONTAINING GAS DIFFUSER LAYER

To prepare the gas diffuser layer, UC 225 IM carbon fiber fabric (e-composites) was cut into a rectangle with an area of approximately 180 cm^2 to cover the faces of the ceramic cup of approximately 200 mL. For this, the procedure of Santoro et al.. (2011) was followed. In this bias, a mixture of 0.7 g of black carbon particles (Vulcan XC-72R), 9.1 mL of distilled water, and 21.5 mL of Triton X100 (Sigma-Aldrich) was prepared and mixed for 1 hour. Soon after, 1 g of PTFE (60% emulsion, Sigma-Adrich) was added and mixed for another 30 minutes. This was added to the ultrasound bath for 15 minutes, followed by mixing by stirring for another 5 minutes, repeating 2 times both the ultrasound bath and the stirring. Then, another 2.75g of *carbon black* was added and mixed for another 1 hour. With this, the mixture was added to one of the faces of the carbon fiber fabric that was heated between two plates for 30 minutes at a temperature of 280 C and then 343 C for 2.5 hours. After cooling, these carbon fabrics were braided with AWG 26 nickel chromium wire, the treated face was added on the ceramic so that it was in contact with the atmospheric air while the untreated face was in contact with the ceramic, these nickel wires were braided to assist in the contact of the fabric with the ceramic and to perform the measurements with the multimeter.

For the cathodes containing Fe-N-C hydrogel, the same procedure was performed, replacing the black carbon with the powder obtained according to the procedure described in subchapter 6.1.

CONSTRUCTION OF THE MICROBIAL BIOFUEL CELL.

The biocells were constructed using ceramic cups of approximately 200 mL, and these ceramics were coated both internally and externally with UC 225 IM carbon fiber fabric (e-composites). The inner carbon fiber fabric, in contact with the ground, will act as

the anode, and the carbon fabric treated with a gas diffuser layer with or without the Fe-N-C hydrogel as the cathode.

In the constructive, both treated coatings were in contact with atmospheric oxygen, as shown in Figure 8. this treatment with different components (gas diffuser layer and Fe-N-C hydrogel incorporated into the gas diffuser layer) was the modified variable in the experiment. For both internal and external coatings, nickel chromium wire was traced to give stability to the fabric in the ceramic and allow the electrical connections to perform the electrochemical measurements.

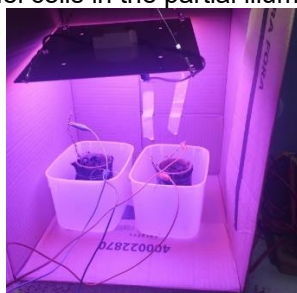
Figure 8 - Cathode already inserted in the BCMs, from left to right: gas diffuser layer and Fe-N-C hydrogel catalyst incorporated into the gas diffuser layer.



Source: Authorship, 2025.

In this bias, 240 g of clay soil not previously cultivated was added to each ceramic, with the following characteristics: organic matter, OM 6 g/dm³; pH, in CaCl₂ - 4.2; Presin – 5 mg/dm³; Potassium – 0.4; Calcium-3; Magnesium-1; CRC-26%, Hydrogen + Aluminum – 22; v%- 16 (FCA- UNESP, 2024), collected at the Federal Institute of São Paulo - Avaré, at the following coordinates -23.078095,-48.927018. Soon after, 15 g of *Sphagnum* moss was inserted into each biocell. These mosses were already developed, so they were already green in color. Then, 100 mL of 100 mM KCl solution was added as electrolyte and taken to the partial illumination chamber, as shown in Figure 9.

Figure 9 - Biofuel cells in the partial illumination chamber.



Source: Authorship, 2025.

ELECTROCHEMICAL EXPERIMENTS

To construct the polarization curves, which is one of the main parameters for measuring the efficiency of the biocell, potential measurements were continuously carried out with the multimeter instrument, varying 15 different resistors with resistances (R) of 1 MΩ, 560 KΩ, 470 KΩ, 220 KΩ, 100 KΩ, 56 KΩ, 10 KΩ, 1KΩ, 560 Ω, 330 Ω, 100 Ω, 56 Ω, 47 Ω, 10 Ω and 1 Ω, always measuring and waiting for stabilization for 2 minutes to obtain the potential difference (V) between the cathode and the anode. Subsequently, by the OHN law (equation 1), the current value (i) was obtained, and with the help of Exel, it was possible to sketch the graphs, consequently visualizing the polarization curves, in addition to plotting the maximum power (P) (equation 2).

$$V = R \cdot i \quad (\text{Equation 1})$$

$$P = V \cdot i \quad (\text{Equation 2})$$

The half-cell experiments were performed using an AUTOLAB potentiostat PGSTAT302. For this, the working electrode (red connection) was connected directly to the anode inside the ceramic cell, a platinum plate was added to the ground (black connection), and an Ag/AgCl reference electrode was added to the soil (blue connection) near the anode (Figure 10). The electrolyte was 0.1M KCl solution. All connections were evaluated with a multimeter to make sure that there was no contact between the electrodes to avoid short circuits and potential *overload*.

Figure 10 – Experiments in half cell for developed electrochemical cell. The anode as the working electrode, a platinum plate as the counter electrode, and an Ag/AgCl reference electrode were used for the potential measurements.



Source: Authorship, 2025.

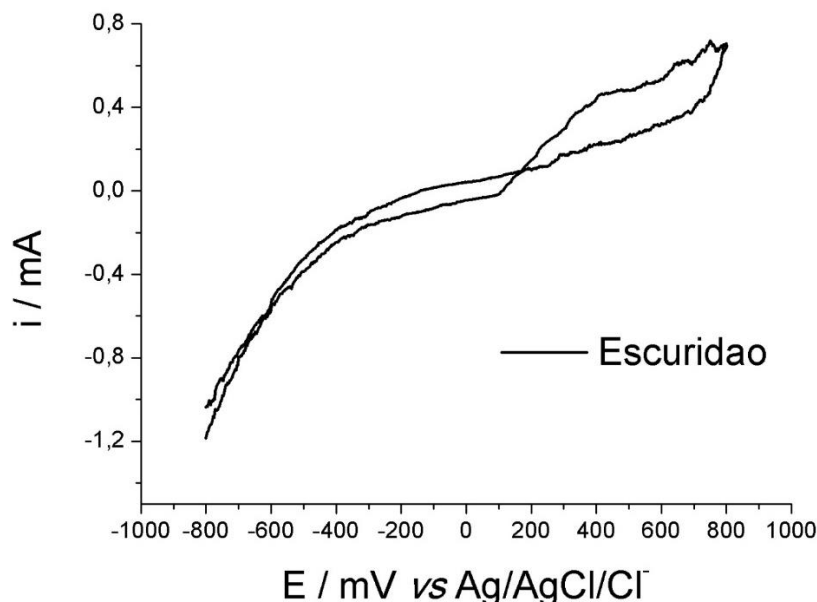
Cyclic voltammetry experiments were conducted in the potential range of 800 to -800 mV vs Ag/AgCl, starting from the open circuit potential and under scanning speed at 10 mV/s. The scanning cycles were repeated until the pseudostationary state was reached, characterized by the absence of significant changes in the voltammogram.

RESULTS AND DISCUSSIONS

HALF-CELL BIOANODE EXPERIMENTS UNDER ILLUMINATION AND DARKNESS

To begin to investigate the faradaic processes occurring on the surface of the electrodes in studies, half-cell experiments were carried out with the electrochemical cell developed in the partial stage. To do this, the carbon tissue added to the inner region of the electrochemical cell was connected as a working electrode to a potentiostat. Cyclic voltammetry experiments were performed with the electrochemical cell in partial illumination and complete darkness using a platinum foil as a counter electrode, and the potentials were measured concerning an Ag/AgCl reference electrode. Figure 11 shows the experiments carried out under total darkness.

Figure 11 – Cyclic voltamogram of the anode in the ceramic electrochemical cell. Experiments were carried out on soil containing mosses *Sphagnum* with 100 mM solution of KCl at 10 mV/s under darkness. The 10th cycle is presented.



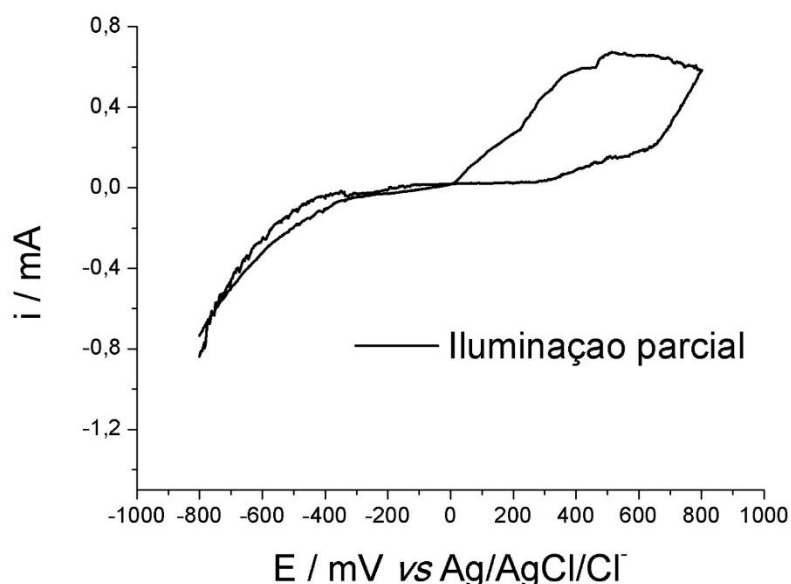
Source: Authorship, 2025.

The cyclic voltammetry experiments with the ceramic electrochemical cell containing soil and *Sphagnum* mosses and KCl solution in a dark environment present a voltammogram with considerable resistivity, observed by the inclination of the entire voltammogram. An oxidation peak starting around 100 mV vs Ag/AgCl is observed, but

without a well-defined peak, as is expected by a process containing all reagent consumption on the electrode surface.

The same electrochemical cell was left under lighting conditions for 1 hour, and the cyclic voltammetry electrochemical experiments were again performed (Figure 12).

Figure 12 – Cyclic voltamogram of the anode in the ceramic electrochemical cell. Experiments were carried out on soil containing mosses *Sphagnum* with 100 mM solution of KCl at 10 mV/s under illumination. The 10th cycle is presented.



Source: Authorship, 2025.

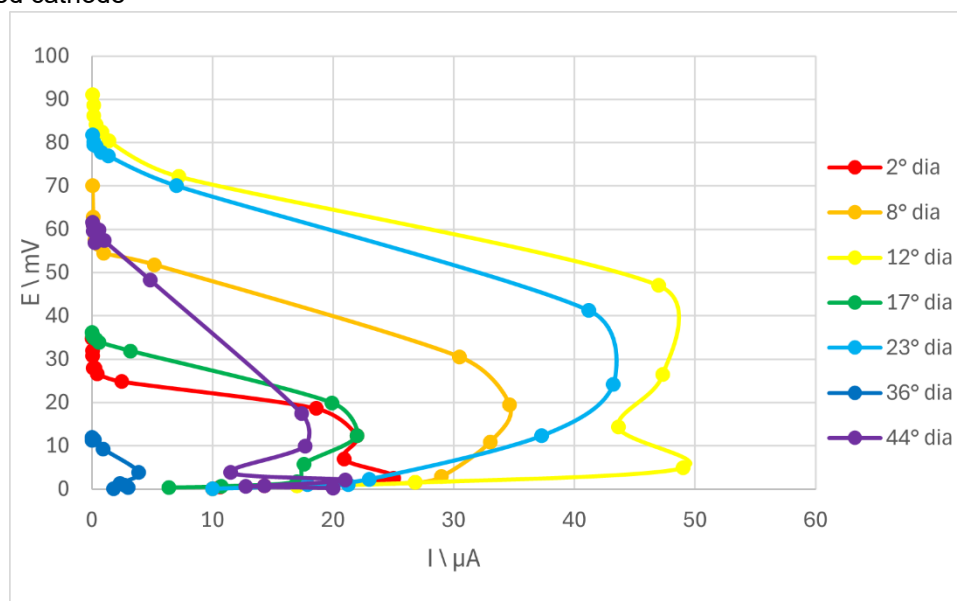
Observing the voltamlogram shown in Figure 12, with the electrochemical cell under illumination, it is possible to observe the beginning of the oxidation peak starting close to 0 mV vs Ag/AgCl. Different from what was observed in Figure 11 with the experiment under lighting, the voltamhogram in Figure 12 under lighting indicates a faradaic process involving a much larger amount of charge since the area under the curve is considerably larger. In addition, a slight deviation from the beginning of the oxidation process is observed at 50 mV.

Cyclic voltammetry experiments suggest that there is production of electroactive compounds that are oxidizing on the surface of the electrode. The lighting offers a positive effect on these compounds, which are produced in greater quantities than the same in dark conditions, converging with the results obtained in the partial stage of this project.

ELECTROCHEMICAL EXPERIMENTS CATHODE TREATED WITH HYDROGEL CATALYST FE-N-C

The polarization curves referring to the electrochemical experiment of ceramic microbial fuel biocells with *Sphagnum* mosses using low-cost cathode based on Fe-N-C hydrogel can be seen in Figure 13.

Figure 13 - Polarization Curves Ceramic Microbial Fuel Biocells with Mosses *Sphagnum* using Fe-N-C hydrogel-based cathode



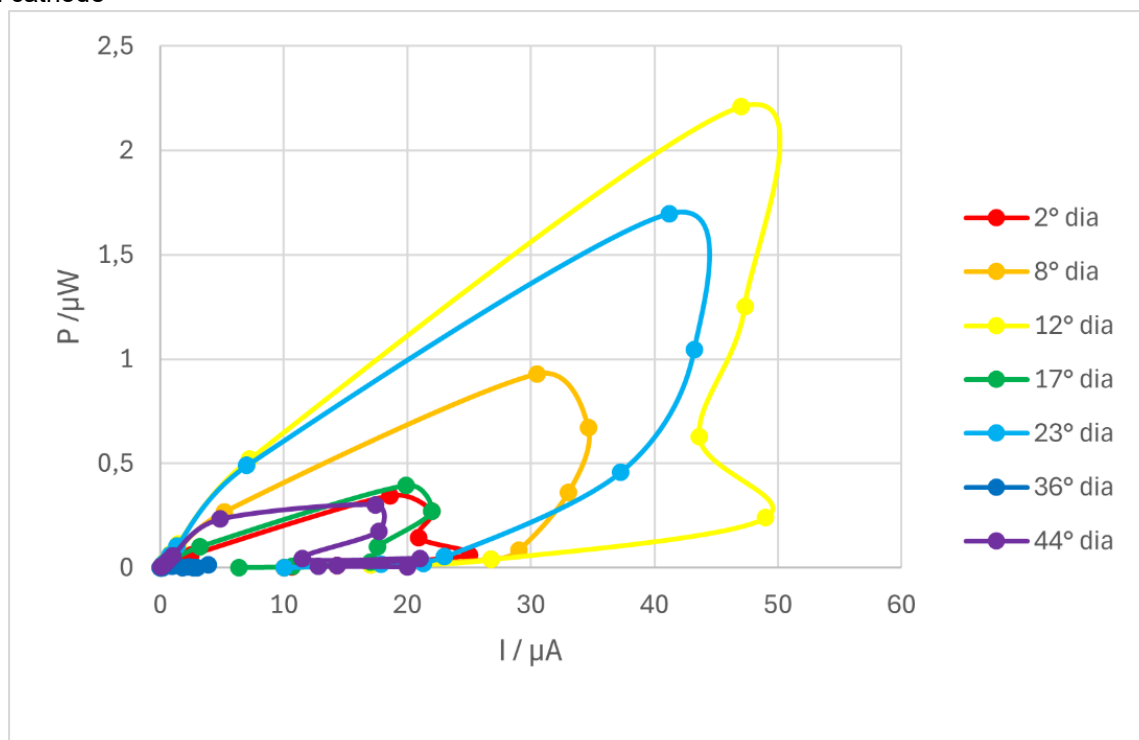
Source: Authorship, 2025.

Each polarization curve depicted above has a color corresponding to a specific day of the measurement, as indicated in the legend on the right. On the 2nd day (red), the open-circuit potential values were 30.7 mV, with the maximum current of 25 μA . On the 8th day (orange), the curve expands significantly from the 2nd day, reaching a maximum open-circuit potential of 70 mV and a maximum current of about 34.6 μA . The 12th day measurement (light yellow) was the day that the biocell recorded the highest performance, with a potential reaching 91.1 mV, while the electric current reached 49 μA . After 17 days (green), the curve decayed and became similar to the beginning of the experiment; the open circuit potential values reached 36.1 mV, with the current reaching about 21.9 μA . The 23rd day (light blue) was the day that the second highest performance was recorded in the measured period, with a potential reaching 81.7 mV and a current close to 43 μA . The 36th day (dark blue) was the day on which the device recorded the lowest performance, with a maximum potential of 11.3 mV and a current of 3.9 μA .

Finally, on the 44th day (purple), the curve shows a significant increase compared to the 36th day, with values similar to the 8th day, with the maximum potential being 61.6 mV and current of 21 μA .

With these data, calculations were performed to determine the maximum power generated each day, as shown in Figure 14.

Figure 14 - Power curves, ceramic microbial fuel biocells with mosses *Sphagnum* using a Fe-N-C hydrogel-based cathode



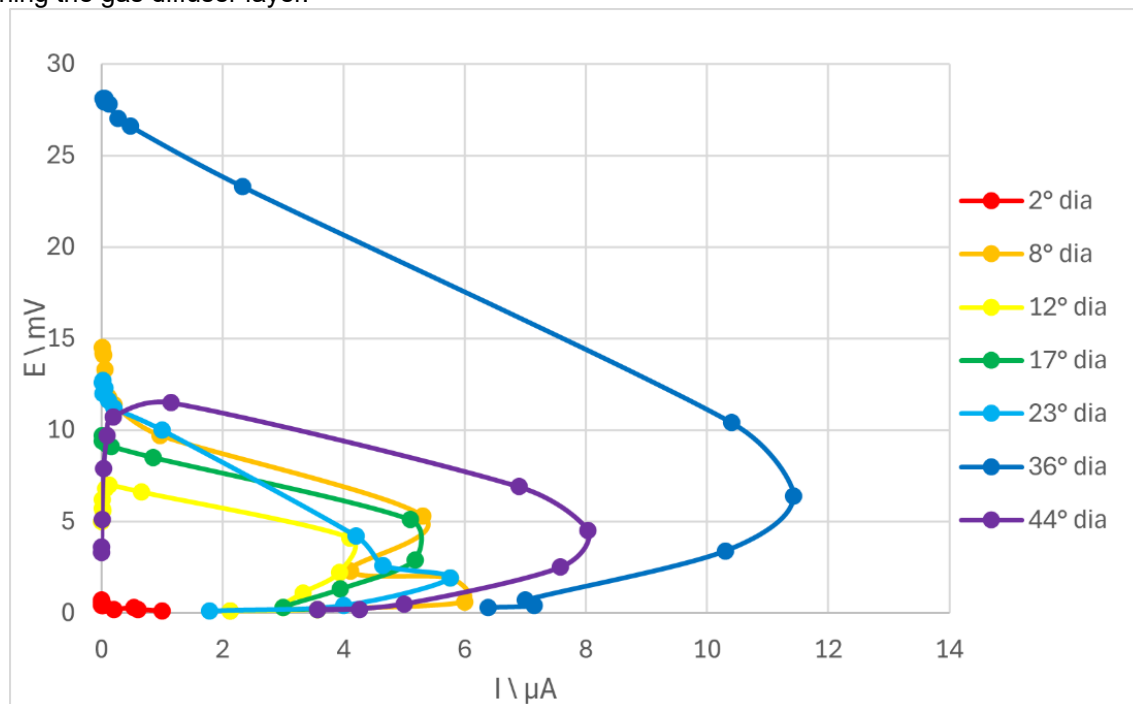
Source: Authorship, 2025.

As can be seen in the image above, the highest potential recorded occurred on the 12th day of the experiment, reaching 2.209 mW, followed by the 23rd day, with a maximum power of 1.69 mW. These were the two days in which the *Sphagnum* moss microbial fuel biocell, with a cathode containing Fe-N-C hydrogel, showed its best performance.

ELECTROCHEMICAL EXPERIMENTS CATHODE WITH GAS DIFFUSER LAYER

The polarization curves referring to the electrochemical experiment of ceramic microbial fuel biocells with *Sphagnum* mosses with cathode containing the gas diffuser layer can be seen in Figure 15.

Figure 15 – Polarization curves of ceramic microbial fuel biocells with mosses *Sphagnum* with cathode containing the gas diffuser layer.

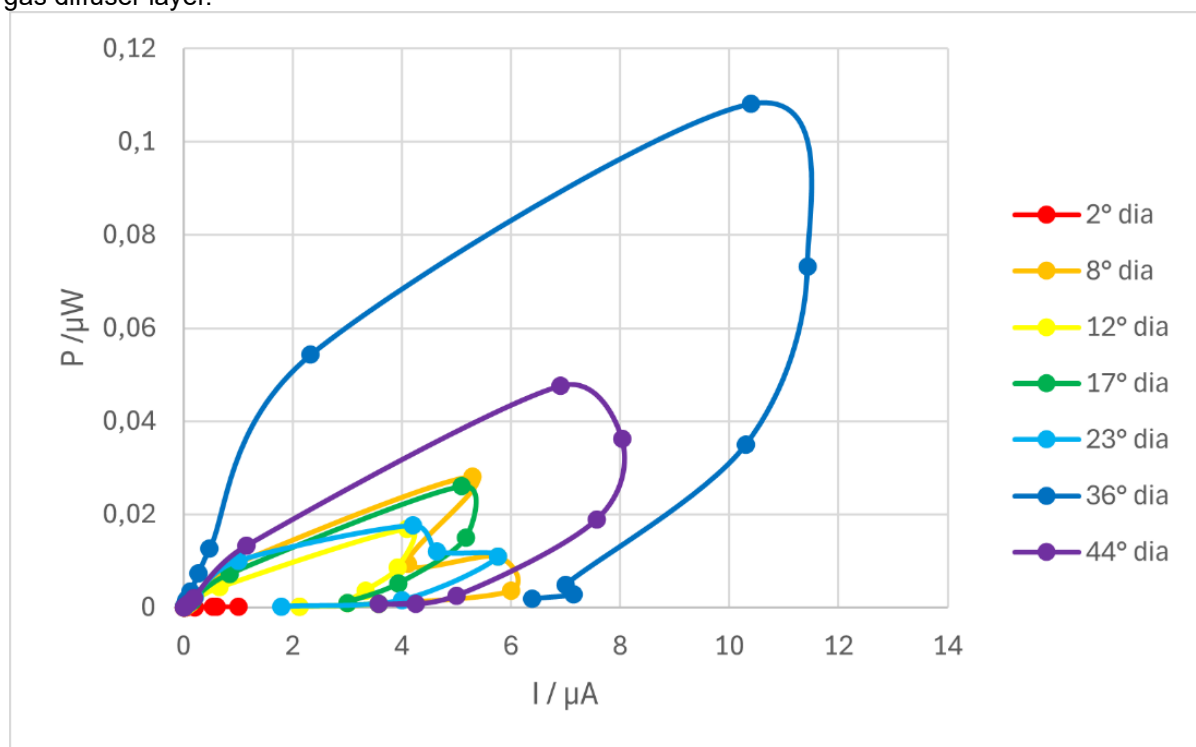


Source: Authorship, 2025.

Each polarization curve depicted above has a color corresponding to a specific day of the measurement, as indicated in the legend on the right. On the 2nd day (red), the open circuit potential values ranged between 0.1 mV and 0.7 mV, with a maximum current of 0.6 μ A, which were the lowest values recorded during the experimental period. On the 8th day (orange), the curve showed a significant expansion compared to the 2nd day, reaching a maximum open-circuit potential of 14.5 mV and a maximum current of about 6 μ A. On the 12th day measurement (light yellow), it registered a decline compared to the 8th day, with the potential reaching 6.6 mV and the electric current reaching 4.1 μ A. After 17 days of experiment (green), there was a small increase in performance compared to the previous measurement, with the curve returning to a measurement pattern similar to the 8th day, the open circuit potential reached 9.7 mV, while the current reached about 5.2 μ A. On the 23rd day (light blue), the measurements remained close to the previous measurements. On the 36th day (dark blue), the device showed its best performance, with a maximum potential of 28.1 mV and a current of 11.4 μ A. Finally, on the 44th day (purple), there was a significant drop compared to the 36th day, with the maximum potential recorded of 11.5 mV, with a current of 8 μ A.

Based on the data obtained, the calculations to determine the maximum power generated on each day were performed (product between voltage and current), the results of which are shown in Figure 16.

Figure 16 - Power curves of ceramic microbial fuel biocells with mosses *Sphagnum* with cathode containing the gas diffuser layer.



Source: Authorship, 2025.

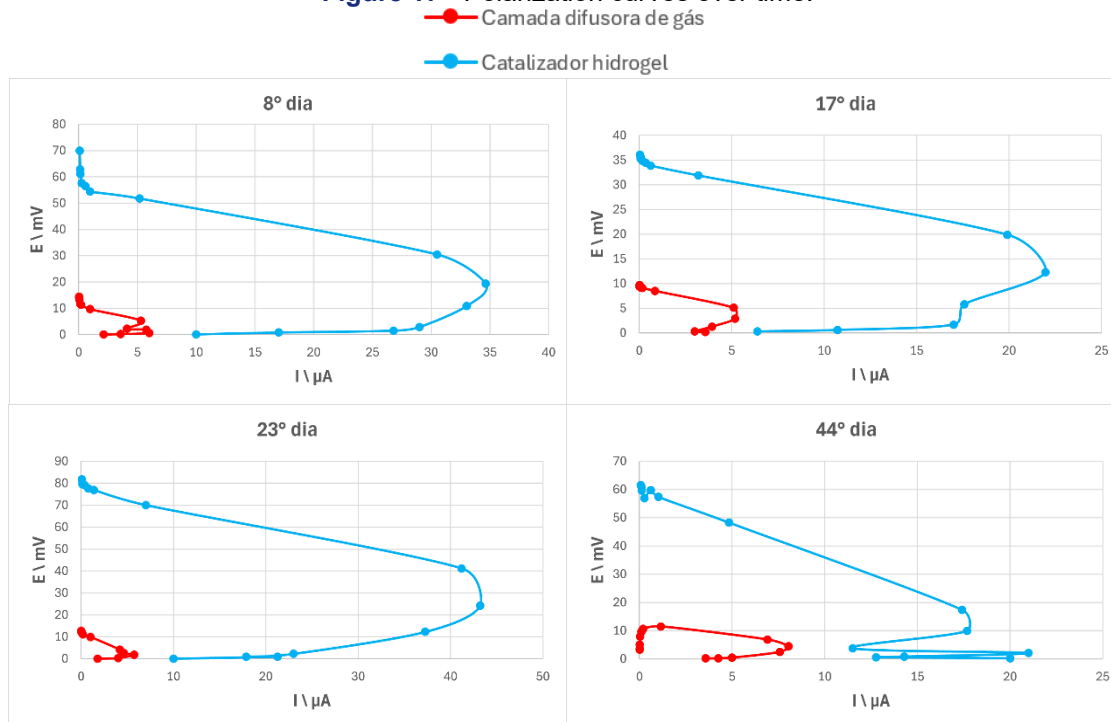
Looking at the data plotted in the graph above (figure 16), the days that presented the highest power is proportional to the days with the best performances about the values of the polarization curves. Therefore, the highest power recorded was on the 36th day with 0.10816 mW, followed by the 44th day with 0.04761 mW.

TEMPORAL EVOLUTION OF MAXIMUM CURRENT, OPEN CIRCUIT POTENTIAL, AND MAXIMUM POWER

Polarization curves play a key role in evaluating the electrochemical performance of a microbial biocell (BCM), as they illustrate the relationship between current density and the potential generated by the cell. These curves provide valuable information on energy efficiency, losses associated with phenomena such as ohmic resistance, mass transfer or activation limitations, and the dynamic behavior of the cell in the face of variations in operating conditions. By analyzing these curves, it is possible to identify critical points of degradation, optimize operating parameters, and understand the system as a whole.

The temporal evolution of the polarization curves of the developed biofuel cells is presented below. Figure 17 illustrates the variations of these curves over time, comparing the cathodes only with the gas diffuser layer and with the gas diffuser layer containing the Fe-N-C hydrogel-based catalyst.

Figure 17 - Polarization curves over time.



Source: Authorship, 2025.

As can be seen in Figure 17, the polarization curves exhibited distinct behaviors about the values of open circuit potential and current density over time, in addition to showing significant differences between the treatments applied to the cathodes. These differences persisted throughout the experiment, with emphasis on the Sphagnum moss BCM with additional Fe-N-C hydrogel treatment, which presented a significant advantage compared to the Sphagnum moss BCM with a conventional gas diffuser layer.

The analysis of the polarization curves proved significant differences in the values of open circuit potential and current density between the treatments applied to the cathodes. These differences were maintained throughout the experiment, highlighting the Sphagnum moss microbial biocell (BCM) with the addition of Fe-N-C hydrogel, which presented a superior performance about the BCM with a conventional gas diffuser layer. Each region of the polarization curve provides important information about the functioning of the system, these regions are divided into three: the first to low values of electric current, also known as loss by activation, which refers to the highest values of potential about the current, indicating how well the biocatalyst operates, the second region, of intermediate current values, concerns the metabolism of microorganisms, characterized by intermediate electric current and constant potential decay, and the third region of high currents, considered as a zone of loss by mass transport is caused by constructive limitations, so that there is a lack of reagent on the electrode surface (Gonçalves, 2021).

In general terms, it is notorious that the insertion of the Fe-N-C hydrogel in the cathode exerted a significant impact on the polarization curves. This is because the insertion of this variable contributed positively to the reaction and reduction of oxygen (RRO), a determining step for a biocell fuel, especially for measuring the efficiency of the cathode and the system as a whole. Although the RRO is a favorable reaction, its activation energy is high, for this reason the insertion of a catalyst is extremely important, which makes the RRO faster, since the catalyst helps to reduce this activation energy, consequently the performance of the BCM with the best catalyst is more advantageous, as evidenced by the results.

The existing scientific theoretical basis is aligned with the results obtained, validating the trends recorded in the electrochemical system. According to Singh et al. (2014), the authors proved the importance of Fe in the high electrocatalytic activity when they compared the activity and stability of Fe-N-C and C-N x materials in cell tests, in this work the importance of the binding metal was proven, which presented higher activity than the C-N x electrocatalyst. According to Ganesan et al. (2014), their study indicated that iron is a component of an active site, consequently, it increases RRO activity. Similarly, Ganesan and Singh observed the fundamental role of Fe retained in the structure as a constituent of active sites and promote advantageous RRO activity compared without the presence of the metal. Therefore, it is promising to use iron as a transition metal - M- in addition to it being abundant in nature and low cost.

According to the studies of WU, Gang et al. (2011), the performance of M-N-C catalysts (M- transition metal, N- nitrogen and C- carbon) is directly related to the chemical structure that is determined by several factors such as synthesis conditions, carbon support and structure of the atmosphere related to heat treatment. From this perspective, some studies suggest that a simple synthesis by pyrolysis, due to heat treatment, produces iron nanoparticles encapsulated with nitrogen-doped carbon that, according to Varnell et al. (2016), the protected sites adjacent to the iron nanoparticles are responsible for the observed activity and stability of the catalyst.

The methodology used in this study also finds theoretical support in the studies of Yang et al. (2019), proved that the preformation of the Fe(III)-chitosan hydrogel produced a relatively uniform and porous structure, in addition, a uniform distribution of Fe on the surface of the Fe-N-C catalyst was proven, without significant agglomeration, which can potentially make more catalytic sites accessible for the oxygen reduction reaction (RRO), thus improving the overall catalytic performance.

When comparing the biocell containing Fe-N-C hydrogel with the control biocell, which has only the conventional gas diffuser layer, a significant advantage is observed in the polarization curves. Visually, at the end of the experiment, the BCMs showed differences in the appearance of the *Sphagnum* mosses. Previous studies of this group have already shown that moss development is directly related to electrochemical performance, reflected in polarization curves. In the specific case of this experiment, BCM with Fe-N-C hydrogel showed an accumulation of soil on the mosses, as shown in Figure 18, possibly interfering with the absorption of light and, consequently, photosynthesis.

Figure 17 - BCMs from left to right, conventional gas diffuser layer, gas diffuser layer with Fe-N-C hydrogel catalyst



Source: Authorship, 2025.

However, even with this adversity, the electrochemical performance of BCM with Fe-N-C hydrogel was still superior to that of BCM control, evidencing the efficiency of the catalyst. The modified biocell showed higher power density and energy conversion efficiency, showing that the introduction of the catalyst was decisive in overcoming the limitations of the ROR. While the control biocell demonstrated constraints on reaction rate and higher internal resistance, the presence of Fe-N-C ensured a more active and efficient catalytic environment, making this approach highly advantageous for bioelectrochemical applications.

CONCLUSIONS

The cyclic voltammetry experiments on the bioanodes developed in the partial stage indicated a peak of oxidation on the carbon surface, which depends on the luminosity of the cell. In darkness, the oxidation peak is poorly defined and starts near 100 mV vs Ag/AgCl. With the lighting, a larger and better-defined peak can be observed, with a start close to 50

mV vs Ag/AgCl, probably resulting from the bioactive compounds produced by the moss in the soil as a result of the change in lighting.

The assemblies of the BCMs are concluded that they were well constructed since the polarization curves are characteristic of the BCMs found in the literature, with the characteristic regions.

The BCM with *Sphagnum* moss incorporated into the Fe-N-C hydrogel catalyst showed superior performance, achieving the highest open-circuit potential of 91.1 mV and an electric current of 49 μ A. In contrast, the BCM with *Sphagnum* moss and gas diffuser layer obtained significantly lower values, with a maximum potential of 28.1 mV and a current of 11.4 μ A. At the end of the experiment, the BCM with incorporated catalyst was partially covered by soil, which possibly affected photosynthesis and reduced its performance. Still, this configuration maintained superior performance, evidencing the efficiency of the Fe-N-C hydrogel catalyst.

REFERENCES

1. Boas Filho, M. V. (2023). *Bioelectrochemical performance of efficient microorganisms and Sphagnum mosses in bioanodes of microbial fuel biocells for clean energy generation* [Bachelor's thesis, Federal Institute of Education, Science and Technology, Avaré Campus].
2. Bombelli, P., Dennis, R. J., Felder, F., Cooper, M. B., Lyster, D. M. R., Royles, J., Harrison, S. T. L., Smith, A. G., Harrison, C. J., & Howe, C. J. (2016). The electrical output of bryophyte microbial fuel cell systems is sufficient to power a radio or an environmental sensor. *Royal Society Open Science*, 3*(10), 160249. <https://doi.org/10.1098/rsos.160249>
3. Carette, L., Friedrich, K. A., & Stimming, U. (2001). Fuel cells – Fundamentals and applications. *Fuel Cells*, 1*(1), 5–39. [https://doi.org/10.1002/1615-6854\(200105\)1:1<5::AID-FUCE5>3.0.CO;2-G](https://doi.org/10.1002/1615-6854(200105)1:1<5::AID-FUCE5>3.0.CO;2-G)
4. Cooney, M. J., Svoboda, V., Lau, C., Martin, G., & Minteer, S. D. (2008). Enzyme-catalysed biofuel cells. *Energy & Environmental Science*, 1*(3), 320–337. <https://doi.org/10.1039/B809009B>
5. Deng, Q., Li, X., Zou, K., Ling, A., & Logan, B. E. (2010). Power generation using an activated carbon fiber felt cathode in an upflow microbial fuel cell. *Journal of Power Sources*, 195*(4), 1130–1135. <https://doi.org/10.1016/j.jpowsour.2009.08.078>
6. Empresa de Pesquisa Energética. (2024). *Electricity consumption in Brazil*. <https://www.epe.gov.br>
7. Ganesan, S., Leonard, N., & Barton, S. C. (2014). Impact of transition metal on nitrogen retention and activity of iron–nitrogen–carbon oxygen reduction catalysts. *Physical Chemistry Chemical Physics*, 16*(10), 4576–4585. <https://doi.org/10.1039/C3CP54810A>
8. Gomes, A. S. O. (2011). *Development of a microbial fuel cell with pure cultures of Pseudomonas aeruginosa in glycerol culture medium* [Master's dissertation, University of São Paulo].
9. Gonçalves, M. P. (2021). *Characterization of the Cac PEM 500 W of Labmater (UFPR-Setor Palotina) fed to H₂: Obtaining the polarization curve* [Bachelor's thesis, Federal University of Paraná].
10. Gonzalez, E. R. (2000). Eletrocatalise e poluição ambiental. *Química Nova*, 23*(2), 262–266. <https://doi.org/10.1590/S0100-40422000000200015>
11. Gorby, Y. A., Yanina, S., McLean, J. S., & Fredrickson, J. K. (2006). Electrically conductive bacterial nanowires produced by *Shewanella oneidensis* strain MR-1 and other microorganisms. *Proceedings of the National Academy of Sciences*, 103*(30), 11358–11363. <https://doi.org/10.1073/pnas.0604517103>
12. Gula, H., Raza, W., Lee, J., Azam, M., Ashraf, M., & Kim, K. (2021). Progress in microbial fuel cell technology for wastewater treatment and energy harvesting. *Chemosphere*, 281*, 130828. <https://doi.org/10.1016/j.chemosphere.2021.130828>

13. Hanson, A. D., McCarty, D. R., Henry, C. S., Xian, X., Joshi, J., Patterson, J. A., García-García, J. D., Fleischmann, S. D., Tivendale, N. D., & Millar, A. H. (2021). The number of catalytic cycles in an enzyme's lifetime and why it matters to metabolic engineering. **Proceedings of the National Academy of Sciences*, 118*(13), e2023348118. <https://doi.org/10.1073/pnas.2023348118>
14. Lefèvre, M., Proietti, E., Jaouen, F., & Dodelet, J.-P. (2009). Iron-based catalysts with improved oxygen reduction activity in polymer electrolyte fuel cells. **Science*, 324*(5923), 71–74. <https://doi.org/10.1126/science.1170051>
15. Logan, B. E. (2008). **Microbial fuel cells**. Wiley & Sons.
16. Logan, B. E., & Regan, J. M. (2006). Electricity-producing bacterial communities in microbial fuel cells. **Trends in Microbiology*, 14*(12), 512–518. <https://doi.org/10.1016/j.tim.2006.10.003>
17. Mesquita, D. V. (2016). **Production of electricity in a microbiological fuel cell with dredging sediment from the Port of Rio Grande** [Master's dissertation, Federal University of Rio Grande].
18. Mineva, T., Matanovic, I., Atanassov, P., Sougrati, M.-T., Stievano, L., Clémancey, M., Kochem, A., Latour, J.-M., & Jaouen, F. (2019). Understanding active sites in pyrolyzed Fe-N-C catalysts for fuel cell cathodes by bridging density functional theory calculations and ⁵⁷Fe Mössbauer spectroscopy. **ACS Catalysis*, 9*(10), 9359–9371. <https://doi.org/10.1021/acscatal.9b02077>
19. Moraes, P. S. (2016). **Energy production in a fluidized bed microbial fuel cell** [Master's dissertation, Federal University of Rio Grande].
20. Neto, S. A., & Andrade, A. R. (2013). New energy sources: The enzymatic biofuel cell. **Journal of the Brazilian Chemical Society*, 24*(12), 1891–1912. <https://doi.org/10.5935/0103-5053.20130237>
21. Oliveira, F. E. R. de. (2018). **Synthesis and investigation of the activity of electrocatalysts formed by MNC-type abundant elements for the oxygen reduction reaction** [Doctoral dissertation, University of São Paulo].
22. Oliveira, R. L. S. (2019). **Prospection of bacteria in the microbiota of soils with energy production capacity** [Bachelor's thesis, Federal University of Ceará].
23. Park, D. H., & Zeikus, J. G. (2003). Improved fuel cell and electrode designs for producing electricity from microbial degradation. **Biotechnology and Bioengineering*, 81*(3), 348–355. <https://doi.org/10.1002/bit.10466>
24. Santoro, C., Lei, Y., Li, B., & Cristiani, P. (2012). Power generation from wastewater using single chamber microbial fuel cells (MFCs) with platinum-free cathodes and pre-colonized anodes. **Biochemical Engineering Journal*, 62*, 8–16. <https://doi.org/10.1016/j.bej.2011.12.006>
25. Santos, F. A. C. M., & Santos, F. M. S. M. (2004). Fuel cells. **Millenium*, (29)*, 146–156.

26. Santos, R. M., Oliveira, L. P., & Costa, A. F. (2023). Environmental impacts of energy generation from fossil fuels. **Brazilian Journal of Renewable Energies*, 12*(3), 45–60. <https://www.revistaenergiasrenovaveis.com.br>
27. Schröder, U. (2007). Anodic electron transfer mechanisms in microbial fuel cells and their energy efficiency. **Physical Chemistry Chemical Physics*, 9*(21), 2619–2629. <https://doi.org/10.1039/B703627G>
28. Shlosberg, Y., Schuster, G., & Adir, N. (2023). Photosynthetic fuel cells: Just an interesting concept or a promise for future technology? **Bioelectricity*, 5*(2), 132–138. <https://doi.org/10.1089/bioe.2023.0005>
29. Shukla, A. K., Suresh, P., Berchmans, S., & Rajendran, A. (2004). Biological fuel cells and their applications. **Current Science*, 87*(4), 455–468.
30. Singh, D., & et al. (2014). A comparison of N-containing carbon nanostructures (CNx) and N-coordinated iron–carbon catalysts (FeNC) for the oxygen reduction reaction in acidic media. **Journal of Catalysis*, 317*, 30–43. <https://doi.org/10.1016/j.jcat.2014.06.006>
31. Teleken, J. T., Silva, J. S., Fraga, M. F., Ogradowski, C. S., Santana, F. B., & Carciofi, B. A. M. (2017). Mathematical modeling of the electric current generation in a microbial fuel cell inoculated with marine sediment. **Brazilian Journal of Chemical Engineering*, 34*(1), 211–225. <https://doi.org/10.1590/0104-6632.20170341s20150462>
32. Ticianelli, E. A., & Gonzalez, E. R. (1989). Fuel cells: A promising alternative for electricity generation. **Química Nova*, 12*(3), 269–270.
33. United Nations. (n.d.). **2030 Agenda for Sustainable Development. Sustainable Development Goal 7: Affordable and clean energy**. <https://www.un.org/sustainabledevelopment/energy/>
34. Varnell, J. A., & et al. (2016). Identification of carbon-encapsulated iron nanoparticles as active species in non-precious metal oxygen reduction catalysts. **Nature Communications*, 7*(1), 12582. <https://doi.org/10.1038/ncomms12582>
35. Wendt, H., Götz, M., & Linardi, M. (2000). Fuel cell technology. **Química Nova*, 23*(4), 538–546. <https://doi.org/10.1590/S0100-40422000000400019>
36. Wu, G., & et al. (2011). Synthesis of nitrogen-doped onion-like carbon and its use in carbon-based CoFe binary non-precious-metal catalysts for oxygen-reduction. **Carbon*, 49*(12), 3972–3982. <https://doi.org/10.1016/j.carbon.2011.05.039>
37. Wu, G., & et al. (2016). Carbon nanocomposite catalysts for oxygen reduction and evolution reactions: From nitrogen doping to transition-metal addition. **Nano Energy*, 29*, 83–110. <https://doi.org/10.1016/j.nanoen.2016.06.018>
38. Yang, W., Wang, X., Rossi, R., & Logan, B. E. (2020). Low-cost Fe–N–C catalyst derived from Fe(III)-chitosan hydrogel to enhance power production in microbial fuel cells. **Chemical Engineering Journal*, 380*, 122522. <https://doi.org/10.1016/j.cej.2019.122522>



39. Zilli, J. É., & et al. (2003). Microbial diversity as an indicator of soil quality. *Cadernos de Ciência & Tecnologia, 20*(3), 391–411.